PART V

SENSOR NETWORKING

20

WIRELESS SENSOR NETWORKS WITH ENERGY HARVESTING

Stefano Basagni, M. Yousof Naderi, Chiara Petrioli, and Dora Spenza

ABSTRACT

This chapter covers the fundamental aspects of energy harvesting-based wireless sensor networks (EHWSNs), ranging from the architecture of an EHWSN node and of its energy subsystem, to protocols for task allocation, MAC, and routing, passing through models for predicting energy availability. With the advancement of energy harvesting techniques, along with the development of small factor harvester for many different energy sources, EHWSNs are poised to become the technology of choice for the host of applications that require the network to function for years or even decades. Through the definition of new hardware and communication protocols specifically tailored to the fundamentally different models of energy availability, new applications can also be conceived that rely on "perennial" functionalities from networks that are truly self-sustaining and with low environmental impact.

20.1 INTRODUCTION

Wireless sensor networks (WSNs) have played a major role in the research field of multihop wireless networks as enablers of applications ranging from environmental and structural monitoring to border security and human health control. Research within this field has covered a wide spectrum of topics, leading to advances in node

Mobile Ad Hoc Networking: Cutting Edge Directions, Second Edition. Edited by Stefano Basagni, Marco Conti, Silvia Giordano, and Ivan Stojmenovic.

hardware, protocol stack design, localization and tracking techniques, and energy management [1].

Research on WSNs has been driven (and somewhat limited) by a common focus: energy efficiency. Nodes of a WSN are typically powered by batteries. Once their energy is depleted, the node is "dead." Only in very particular applications can batteries be replaced or recharged. However, even when this is possible, the replacement/recharging operation is slow and expensive and decreases network performance. Different techniques have therefore been proposed to slow down the depletion of battery energy, which include power control and the use of *duty cycle*-based operation. The latter technique exploits the low power modes of wireless transceivers, whose components can be switched off for energy saving. When the node is in a low power (or "sleep") mode its consumption is significantly lower than when the transceiver is on [2,3]. However, when asleep the node cannot transmit or receive packets. The duty cycle expresses the ratio between the time when the node is on and the sum of the times when the node is on and asleep. Adopting protocols that operate at very low duty cycles is the leading type of solution for enabling long-lasting WSNs [4]. However, this approach suffers from two main drawbacks. (1) There is an inherent tradeoff between energy efficiency (i.e., low duty cycling) and data latency, and (2) battery operated WSNs fail to provide the needed answer to the requirements of many emerging applications that demand network lifetimes of decades or more. Battery leakage and aging depletes batteries within a few years, even if they are seldom used [5,6]. For these reasons, recent research on long-lasting WSNs is taking a different approach, proposing *energy harvesters* combined with the use of rechargeable batteries and super-capacitors (for energy storage) as the key enabler to "perpetual" WSN operations.

Energy-Harvesting-based WSNs (EHWSNs) are the result of endowing WSN nodes with the capability of extracting energy from the surrounding environment. Energy harvesting can exploit different sources of energy, such as solar power, wind, mechanical vibrations, temperature variations, magnetic fields, and so on. By continuously providing energy and storing it for future use, energy harvesting subsystems enable WSN nodes to last potentially forever.

This chapter explores the opportunities and challenges of EHWSNs, explaining why the design of protocol stacks for traditional WSNs has to be radically revisited. We start by describing the architecture of a EHWSN node, and especially that of its energy subsystem (Section 20.2). We then present the various forms of energy that are available and ways for harvesting them (Section 20.3). Models for predicting availability of wind and solar energy are described in Section 20.4. We then survey task allocation, MAC, and routing protocols proposed so far for EHWSNs in Section 20.5.

20.2 NODE PLATFORMS

EHWSNs are composed of individual nodes that, in addition to sensing and wireless communications, are capable of extracting energy from multiple sources and converting it into usable electrical power. In this section we describe in detail the architecture

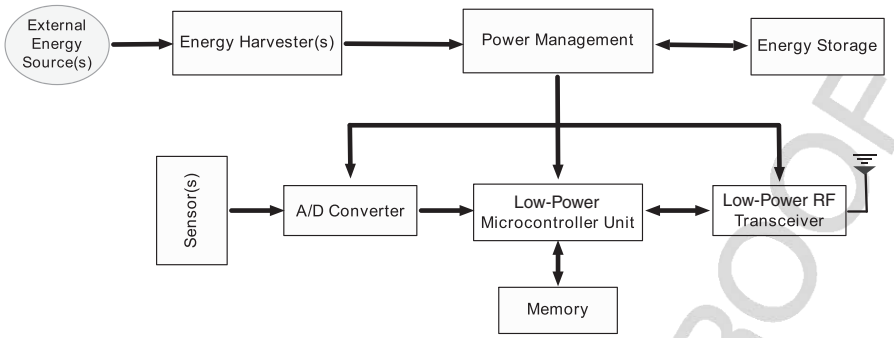

Figure 20.1 System architecture of a wireless node with energy harvesters.

of a wireless sensor node with energy harvesting capabilities, including models for the harvesting hardware and for batteries.

20.2.1 Architecture of a Sensor Node with Harvesting Capabilities

The system architecture of a wireless sensor node includes the following components (Figure 20.1): (1) the energy harvester(s), in charge of converting external ambient or human-generated energy to electricity; (2) a power management module, which collects electrical energy from the harvester and either stores it or delivers it to the other system components for immediate usage; (3) energy storage, for conserving the harvested energy for future usage; (4) a microcontroller; (5) a radio transceiver, for transmitting and receiving information; (6) sensory equipment; (7) an A/D converter to digitize the analog signal generated by the sensors and makes it available to the microcontroller for further processing, and (8) memory to store sensed information, application-related data, and code.

In the next section we focus on the energy harvesting components (the energy subsystem) of a EHWSN node, describing abstractions that have been proposed for modeling them.

20.2.2 Harvesting Hardware Models

The general architecture of the energy subsystem of a wireless sensor node with energy harvesting capabilities is shown in Figure 20.2.

The energy subsystem includes one or multiple harvesters that convert energy available from the environment to electrical energy. The energy obtained by the harvester may be used to directly supply energy to the node or it may be stored for later use. However, in some applications it is possible to directly power the sensor node using the harvested energy, with no energy storage (*harvest-use* architecture [7]); in general this is not a viable solution. A more reasonable architecture enables the node to directly use the harvested energy, but also includes a storage component that acts as an energy buffer for the system, with the main purpose of accumulating and preserving

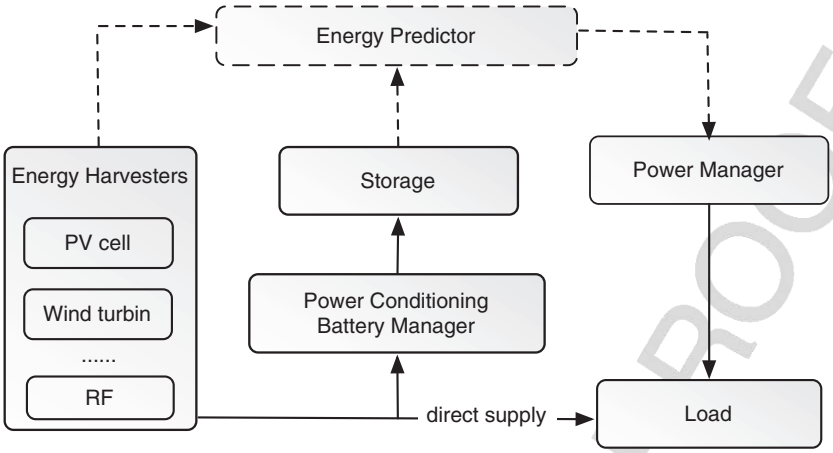

Figure 20.2 General architecture of the energy subsystem of a wireless sensor node with energy harvesting capabilities.

the harvested energy. When the harvesting rate is greater than the current usage, the buffer component can store excess energy for later use (e.g., when harvesting opportunities do not exist), thus supporting variations in the power level emitted by the environmental source.

The two alternatives commonly used for energy storage are *secondary rechargeable batteries* and *super-capacitors* (also known as ultracapacitors). Super-capacitors are similar to regular capacitors, but they offer very high capacitance in a small size. They offer several advantages with respect to rechargeable batteries [8]. First of all, super-capacitors can be recharged and discharged virtually an unlimited number of times, while the typical lifetime of an electrochemical battery is less than 1000 cycles [5]. Second, they can be charged quickly using simple charging circuits, thus reducing system complexity, and do not need full-charge or deep-discharge protection circuits. They also have higher charging and discharging efficiency than electrochemical batteries [8]. Another additional benefit is the reduction of environmental issues related to battery disposal. Thanks to these characteristics, many platforms with harvesting capabilities use super-capacitors as energy storage, either by themselves [9,10] or in combination with batteries [11–13]. Other systems, instead, focus on platforms using only rechargeable batteries [14–16].

Both types of storage devices deviate from ideal energy buffers in a number of ways: They have a finite size B^{Max} and can hold a finite amount of energy, and they have a charging efficiency $\eta_c < 1$ and a discharging efficiency $\eta_d < 1$; that is, some energy is lost while charging and discharging the buffer, and they suffer from leakage and self-discharge; that is, some stored energy is lost even if the buffer is not in use. Leakage and self-discharge are phenomena that affect both batteries and supercapacitors. All batteries suffer from self-discharge: A cell that simply sits on the shelf,

without any connection between the electrodes, experiences a reduction in its stored charge due to internal chemical reactions, at a rate depending on the cell chemistry and the temperature. A similar phenomenon affects electrochemical super-capacitors in charged state. They suffer gradual loss of energy and reduction of the inter-plate voltage. In order to reduce the energy lost trough buffer inefficiencies, many platforms allow the node to directly use the energy harvested. In particular, if the current energy consumption is greater or equal than the energy currently harvested, then the node can use the harvested energy for its operations. This is the most efficient way of using the environmental energy, because it is used directly and there is no energy loss. Otherwise, if the amount of energy harvested is greater than the current energy consumption, some energy is directly used to sustain the node operations, while excess energy is stored in the buffer for later use.

20.2.2.1 Super-Capacitor Leakage Models. Considering leakage current is important while dealing with energy harvesting systems, especially if the application scenario requires the harvested energy to be stored for long periods of time. In general, if the energy source is sporadic or if it is only able to provide a small amount of energy, the portion of the harvested energy lost due to leakage may be significant. The leakage is of particular relevance for super-capacitors, because their energy density is about one order of magnitude lower than that of an electrochemical battery, but they suffer from considerably higher self-discharge. A super-capacitor leakage is strongly variable and depends on several factors, including the capacitance value of the super-capacitor, the amount of energy stored, the operating temperature, the charge duration, etc. For this reason, the leakage pattern of a particular super-capacitor must often be determined experimentally [8,12,17,18]. Additionally, the leakage current varies with time: It is considerably higher immediately after the super-capacitor has been charged, and then it decreases to a plateau.

Several models for the leakage from a charged super-capacitor have been proposed in the literature, modeling the leakage as a constant current [19], or as an exponential function of the current super-capacitor voltage [20], or by using a polynomial approximation of its empirical leakage pattern [18], or, finally, by using a piecewise linear approximation of its empirical leakage pattern [8]. These models have been proposed after experimental observations of actual super-capacitor leakage, such as those shown in Figure 20.3 showing the self-discharge experienced by a charged 25-F super-capacitor over a two-week period.

Another aspect to consider in the super-capacitors versus battery comparison is that in many application scenarios it is not possible to use the full energy stored in the super-capacitor. The voltage of a super-capacitor drops from full voltage to zero linearly, without the flat curve that is typical of most electrochemical batteries. The fraction of the charge available to the sensor node depends on the voltage requirements of the platform. For example, a Telos B mote requires a minimal voltage ranging from 1.8 V to 2.1 V. When the super-capacitor voltage drops below this threshold, its residual energy can no longer be used to power the node. This aspect may be partially mitigated by using a DC–DC converter to increase the voltage range, at the cost of introducing inefficiencies and an additional source of power consumption.

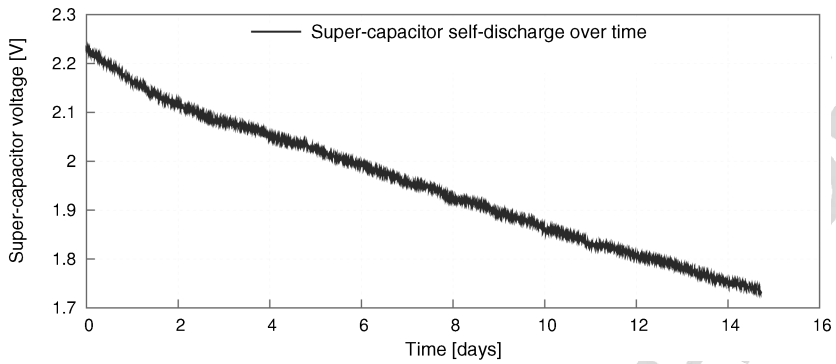

Figure 20.3 Self-discharge of a super-capacitor over time.

20.2.3 Battery Models

Batteries are usually seen as ideal energy storage devices, containing a given amount of energy units. Executing a node operation—for example, sending or receiving a packet—uses a certain amount of energy units, depending on the energy cost of the operation. Battery capacity is assumed to be decreased by the amount of energy required by an operation only when the operation is performed. Real batteries, however, operate differently. As mentioned earlier, all batteries suffer from self-discharge. Even a cell that is not being used experience a charge reduction caused by internal chemical activity. Batteries also have charge and discharge efficiency strictly < 1; that is, some energy is lost when charging and discharging the battery. Additionally, batteries have some nonlinear properties [5,21,22]. These are: (a) *rate-dependent capacity*; that is, the delivered capacity of a battery decreases, in a nonlinear way, as the discharge rate increases; (b) *temperature effect*, in that the operating temperature affects the battery discharge behavior and directly impacts the rate of self-discharge; and (c) *recovery effect*, for which the lifetime and the delivered capacity of a battery increases if discharge and idle periods alternate (pulse discharge). Furthermore, rechargeable batteries experience a reduction of their capacity at each recharge cycle, and their voltage depends on the charging level of the battery and varies during discharge. These characteristics should be taken into account when dimensioning and simulating energy harvesting systems, because they can easily lead to wrong estimations of the battery lifetime. For example, if the harvesting subsystem uses a rechargeable battery to store the energy harvested from the environment, it is important to consider that the reduction in capacity experienced by the battery at each recharge cycle is likely to reduce both its delivered capacity and its lifetime.

Many types of battery models have been proposed recently in the literature [22]. These include: *Physical models* simulate the physical processes that take place into an electrochemical battery. These models are usually very accurate, but have high computational complexity and require high configuration effort [23,24]. *Empirical models* that approximate the discharge behavior of a battery with simple equations. They are

generally the least accurate. However, they require low computational resources and configuration effort [25,26]. *Abstract models* emulate battery behavior by using simplified equivalent representation, such as stochastic systems [27], electrical-circuit models [28,29], and discrete-time VHDL specification [30]; and *mixed models* use both a high-level representation of a battery (simpler than a real battery) and analytic expressions based on low-level analysis and physical laws [31].

20.3 TECHNIQUES OF ENERGY HARVESTING

Figure 20.4 shows the variety of energy types that can be harvested. In this section we provide their brief description and relevant references.

Mechanical energy harvesting indicates the process of converting mechanical energy into electricity by using vibrations, mechanical stress and pressure, strain from the surface of the sensor, high-pressure motors, waste rotational movements, fluid, and force. The principle behind mechanical energy harvesting is to convert the energy of the displacements and oscillations of a spring-mounted mass component inside the harvester into electrical energy [32,33]. Mechanical energy harvesting can be *piezoelectric*, *electrostatic*, and *electromagnetic*.

Piezoelectric energy harvesting is based on the piezoelectric effect for which mechanical energy from pressure, force, or vibrations is transformed into electrical power by straining a piezoelectric material. The technology of a piezoelectric harvester is usually based on a cantilever structure with a seismic mass attached into a piezoelectric beam that has contacts on both sides of the piezoelectric material [33]. In particular, strains in the piezoelectric material produce charge separation across the harvester, creating an electric field, and hence voltage, proportional to the stress generated [34,35]. Voltage varies depending on the strain and time, and an irregular AC

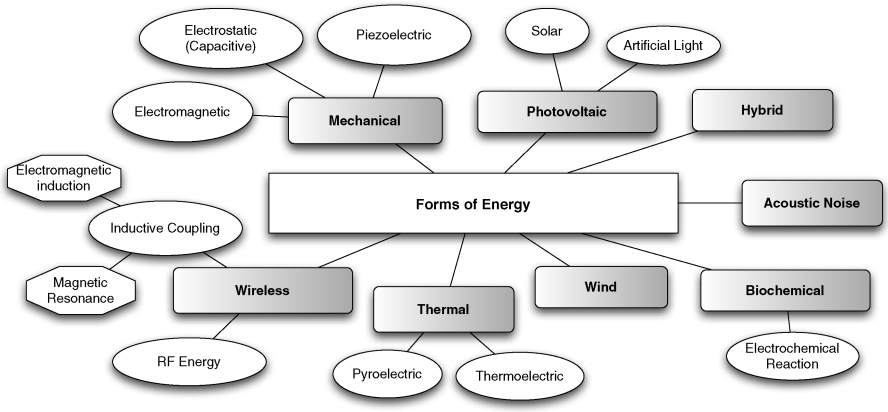

Figure 20.4 Different energy types (rectangles) and sources (ovals).

signal is produced. Piezoelectric energy conversion has the advantage that it generates the desired voltage directly, without need for a separate voltage source. However, piezoelectric materials are breakable and can suffer from charge leakage [33,36,37]. Examples of piezoelectric energy harvesters can be found in references 38–42 and references therein.

The principle of *electrostatic energy harvesting* is based on changing the capacitance of a vibration dependent variable capacitor [43,44]. In order to harvest the mechanical energy, a variable capacitor is created by opposing two plates, one fixed and one moving, and is initially charged. When vibrations separate the plates, mechanical energy is transformed into electrical energy from the capacitance change. This kind of harvester can be incorporated into microelectronic devices due to their integrated circuit-compatible nature [45]. However, an additional voltage source is required to initially charge the capacitor [37]. Recent efforts to prototype sensor-size electrostatic energy harvesters can be found in references 46 and 47.

Electromagnetic energy harvesting is based on Faraday's law of electromagnetic induction. An electromagnetic harvester uses an inductive spring mass system for converting mechanical energy to electrical. It induces voltage by moving a mass of magnetic material through a magnetic field created by a stationary magnet. Specifically, vibration of the magnet attached to the spring inside a coil changes the flux and produces an induced voltage [33,34,43]. The advantages of this method include the absence of mechanical contact between parts and of a separate voltage source, which improves the reliability and reduce the mechanical damping in this type of harvester [36,44]. However, it is difficult to integrate them in sensor nodes because of the large size of electromagnetic materials [36]. Some examples of electromagnetic energy harvesting systems are presented in references 48 and 49.

Photovoltaic energy harvesting is the process of converting incoming photons from sources such as solar or artificial light into electricity. Photovoltaic energy can be harnessed by using photovoltaic (PV) cells. These consist of two different types of semiconducting materials called *n-type* and *p-type*. An electrical field is formed in the area of contact between these two materials, called the P–N junction. Upon exposure to light, a photovoltaic cell releases electrons. Photovoltaic energy conversion is a traditional, mature, and commercially established energy-harvesting technology. It provides higher power-output levels compared to other energy harvesting techniques and is suitable for larger-scale energy harvesting systems. However, its generated power and the system efficiency strongly depend on the availability of light and on environmental conditions. Other factors, including the materials used for the photovoltaic cell, affect the efficiency and level of power produced by photovoltaic energy harvesters [16,36]. Some recent prototypes of photovoltaic harvesters are described in references 50–53. Known implementations of solar energy harvesting sensor nodes include Fleck [54], Enviromote [55], Trio [11], Everlast [10], and Solar Biscuit [56].

Thermal energy harvesting is implemented by *thermoelectric energy harvesting* and *pyroelectric energy harvesting*.

Thermoelectric energy harvesting is the process of creating electric energy from temperature difference (thermal gradients) using thermoelectric power generators (TEGs). The core element of a TEG is a thermopile formed by arrays of two dissimilar

conductors—that is, a *p*-type and *n*-type semiconductor (thermocouple), placed between a hot and a cold plate and connected in series. A thermoelectric harvester scavenges the energy based on the Seebeck effect, which states that electrical voltage is produced when two dissimilar metals joined at two junctions are kept at different temperatures [57]. This is because the metals respond differently to the temperature difference, creating heat flow through the thermoelectric generator. This produces a voltage difference that is proportional to the temperature difference between the hot and cold plates. The thermal energy is converted into electrical power when a thermal gradient is created. Energy is harvested as long as the temperature difference is maintained.

Pyroelectric energy harvesting is the process of generating voltage by heating or cooling pyroelectric materials. These materials do not need a temperature gradient similar to a thermocouple. Instead, they need time-varying temperature changes. Changes in temperature modify the locations of the atoms in the crystal structure of the pyroelectric material, which produces voltage. To keep generating power, the whole crystal should be continuously subject to temperature change. Otherwise, the produced pyroelectric voltage gradually disappears due to leakage current [58].

Pyroelectric energy harvesting achieves greater efficiency compared to thermoelectric harvesting. It supports harvesting from high temperature sources, and it is much easier to get to work using limited surface heat exchange. On the other hand, thermoelectric energy harvesting provides higher harvested energy levels. The maximum efficiency of thermal energy harvesting is limited by the Carnot cycle [43]. Because of the various sizes of thermal harvesters, they can be placed on the human body, on structures and equipment. Some example of this kind of harvesters for WSN nodes are described in [59,60].

Wireless energy harvesting techniques can be categorized into two main categories: *RF energy harvesting* and *resonant energy harvesting*.

RF energy harvesting is the process of converting electromagnetic waves into electricity by a rectifying antenna, or *rectenna*. Energy can be harvested from either (a) ambient RF power from sources such as radio and television broadcasting, cellphones, WiFi communications, and microwaves or (b) EM signals generated at a specific wavelength. Although there is a large amount of potential ambient RF power, the energy of existing EM waves are extremely low because energy rapidly decreases as the signal spreads farther from the source. Therefore, in order to scavenge RF energy efficiently from existing ambient waves, the harvester must remain close to the RF source. Another possible solution is to use a dedicated RF transmitter to generate more powerful EM signals merely for the purpose of powering sensor nodes. Such RF energy harvesting is able to efficiently deliver power ranging from microwatts to few milliwatts, depending on the distance between the RF transmitter and the harvester.

Resonant energy harvesting, also called resonant inductive coupling, is the process of transferring and harvesting electrical energy between two coils, which are highly resonant at the same frequency. Specifically, an external inductive transformer device, coupled to a primary coil, can send power through the air to a device equipped with a secondary coil. The primary coil produces a time-varying magnetic flux that crosses the secondary coil, inducing a voltage. In general, there are two possible

implementations of resonant inductive coupling: weak inductive coupling and strong inductive coupling. In the first case, the distance between the coils must be very small (few centimeters). However, if the receiving coil is properly tuned to match the external powered coil, a "strong coupling" between electromagnetic resonant devices can be established and powering is possible over longer distances. Note that since the primary and secondary coil are not physically connected, resonant inductive coupling is considered a wireless energy harvesting technique. Some recent implementations of wireless energy harvesting techniques for WSNs can be found in references 61–63.

Wind energy harvesting is the process of converting air flow (e.g., wind) energy into electrical energy. A properly sized wind turbine is used to exploit linear motion coming from wind for generating electrical energy. Miniature wind turbines exists that are capable of producing enough energy to power WSN nodes [64]. However, efficient design of small-scale wind energy harvesting is still an ongoing research, challenged by very low flow rates, fluctuations in wind strength, the unpredictability of flow sources, and so on. Furthermore, even though the performance of large-scale wind turbines is highly efficient, small-scale wind turbines show inferior efficiency due to the relatively high viscous drag on the blades at low Reynolds numbers [32,65]. Recent examples of wind energy harvesting systems designed for WSNs include references 13, 64, and 66–68.

Biochemical energy harvesting is the process of converting oxygen and endogenous substances into electricity via electrochemical reactions [69,70]. In particular, biofuel cells acting as active enzymes and catalysts can be used to harvest the biochemical energy in biofluid into electrical energy. Human body fluids include many kinds of substances that have harvesting potential [71]. Among these, glucose is the most common used fuel source. It theoretically releases 24 free electrons per molecule when oxidized into carbon dioxide and water. Even though biochemical energy harvesting can be superior to other energy harvesting techniques in terms of continuous power output and biocompatibility [69], its performance depends on the type and availability of fuel cells. Advantages and disadvantages of using enzymatic fuel cells for energy production are described in reference 72. Research efforts such as references 69, 70, and 73 are examples of recent proposed prototypes that use biochemical energy harvesting to power microelectronic devices.

Acoustic energy harvesting is the process of converting high and continuous acoustic waves from the environment into electrical energy by using an acoustic transducer or resonator. The harvestable acoustic emissions can be in the form of longitudinal, transverse, bending, and hydrostatic waves ranging from very low to high frequencies [74]. Typically, acoustic energy harvesting is used where local long-term power is not available, as in the case of remote or isolated locations, or where cabling and electrical commutations are difficult to use such as inside sealed or rotating systems [74,75]. However, the efficiency of harvested acoustic power is low and such energy can only be harvested in very noisy environments. Harvestable energy from acoustic waves theoretically yields 0.96 $\mu W/cm^3$ [76], which is much lower than what is achievable by other energy harvesting techniques. As such, limited research has been performed to investigate this type of harvesters. Examples of acoustic energy harvesting systems can be found in references 77 and 78.

Table 20.1 Power Density and Efficiency of Energy Harvesting Techniques

Energy Harvesting Technique	Power Density	Efficiency
Photovoltaic	Outdoors (direct sun): 15 mW/cm^2 Outdoors (cloudy day): 0.15 mW/cm^2 Indoors: $<$10 μW/cm^2 [36,37,79,80]	Highest: 32 $\pm$ 1.5% Typical: 25 $\pm$ 1.5% [87]
Thermoelectric	Human: 30 μW/cm^2 Industrial: 1–10 mW/cm^2 [80,81]	$\pm$0.1% $\pm$3% [80]
Pyroelectric	8.64 μW/cm^2 at the temperature rate of 8.5°C/s [82]	3.5% [88]
Piezoelectric	250 μW/cm^3 330 μW/cm^3 (shoe inserts) [36,37]	[a]
Electromagnetic	Human motion: 1–4 μW/cm^3 [67,83] Industrial: 306 μW/cm^3 [84], 800 μW/cm^3 [67]	[a]
Electrostatic	50–100 μW/cm^3 [34]	[a]
RF	GSM 900/1800 MHz: 0.1 μW/cm^2 WiFi 2.4 GHz: 0.01 μW/cm^2 [79]	50%[b] [89]
Wind	380 μW/cm^3 at the speed of 5 m/s [40,85]	5% [40]
Acoustic noise	0.96 μW/cm^3 at 100 dB 0.003 μW/cm^3 at 75 dB [16,86]	[c]

[a]Maximum power and efficiency are source-dependent.
[b]Excluding transmission efficiency.
[c]Noise power densities are theoretical values.

All previously described harvesting techniques can be combined and concurrently used on a single platform (**hybrid energy harvesting**).

A bird's-eye view of the amount of energy harvestable from different sources is given in Table 20.1. For each energy harvesting technique we show its *power density* and *conversion efficiency*. The power density expresses the harvested energy per unit volume, area, or mass. Common unit measures of power density include watts per square centimeter and watts per cubic centimeter. Conversion efficiency is defined as the ratio of the harvested electrical power to the harvestable input power. The energy conversion efficiency is a dimensionless number between 0% and 100%.

20.4 PREDICTION MODELS

Practical use of energy harvesting technologies needs to deal with the variable behavior of the energy sources, which impose the amount and the rate of the harvested energy over time. In case of predictable, noncontrollable power sources, such as the solar one, energy prediction methods can be used to forecast the source availability and estimate the expected energy intake [19]. Such a predictor can alleviate the problem of the harvested power being neither constant nor continuous, allowing the system to take critical decisions about the utilization of the available energy. In this section

we give an overview of the different energy predictors proposed in the literature for two popular forms of energy harvesters, namely, solar and wind harvesters.

EWMA. Kansal et al. [19] propose a solar energy prediction model based on an *Exponentially Weighted Moving-Average* (EWMA) filter [90]. This method is based on the assumption that the energy available at a given time of the day is similar to that available at the same time of previous days. Time is discretized into N timeslots of fixed length (usually 30 minutes each). The amount of energy available in previous days is maintained as a weighted average where the contribution of older data is exponentially decreasing. More formally, the EWMA model predicts that in timeslot n the amount of energy $\mu_n^{(d)} = \alpha \cdot x_n + (1 - \alpha) \cdot \mu_n^{(d-1)}$ will be available for harvesting, where x_n is the amount of energy harvested by the end of the nth slot; $\mu_n^{(d-1)}$ is the average over the previous $d - 1$ days of the energy harvested in their nth slot, and α is a weighting factor, $0 \leq \alpha \leq 1$. EWMA exploits the diurnal solar energy cycle and adapts to seasonal variations. The prediction results very accurate in presence of scarce weather variability. However, when weather conditions are frequently changing (e.g., a mix of sunny and cloudy days in a row), EWMA does not adapt well to the variations in the solar energy profile.

WCMA. The prediction method *Weather-Conditioned Moving Average*, or WCMA for short, has been proposed by Piorno et al. [91] for addressing the shortcomings of EWMA. Similarly to EWMA, WCMA takes into account energy harvested in the previous days. However, it also consider the weather conditions of the current and of the previous days. Specifically, WCMA stores a matrix E of size $D \times N$, where D is the number of days considered and N is the number of timeslots per day. The entry $E_{d,n}$ stores the energy harvested in day d at timeslot n. Energy in the current day is kept in a vector C of size N. In addition, WCMA keeps a vector M of size N whose nth entry M_n stores the average energy observed during timeslot n in the last D days:

$$M_n = \frac{1}{D} \cdot \sum_{i=1}^{D} E_{d-i,n}$$

At the end of each day, M is updated with the energy just observed, overwriting the date of the previous day. The amount of energy P_{n+1} predicted by WCMA for the next timeslot $n + 1$ of the current day is computed as $\alpha \cdot C_n + (1 - \alpha) \cdot M_{n+1} \cdot GAP_n^K$, where C_n is the amount of energy observed during timeslot n of the current day; M_{n+1} is the average of the energy harvested during timeslot $n + 1$ over the last D days; GAP_n^K is a weighting factor providing an indication of the changing weather conditions during timeslot n of the current day with respect to the previous D days, and α is a weighting factor, $0 \leq \alpha \leq 1$. In case of frequently changing weather conditions, WCMA is shown to obtain average prediction errors almost 20% smaller than EWMA.

An enhanced version of WCMA has been presented by Bergonzini et al. [92]. The authors noticed that the prediction error of WCMA shows characteristic peaks at sunrise and at sunset, especially for values of $\alpha > 0.5$. This is because WCMA

considers the value observed in the previous slot for energy predictions. Since at sunrise and sunset the solar conditions changes significantly, this leads to higher prediction errors. In order to address the issue, the authors propose to use a feedback mechanism, called *phase displacement regulator*, providing a sensible decrease of the WCMA prediction error.

ETH Predictor. Moser et al. [93] of ETH Zurich propose a prediction method based on a weighted sum of historical data The ETH prediction algorithm assumes solar power to be periodic on a daily basis. As in previous approaches, time is partitioned into timeslots of fixed length T (in practice lasting from a few minutes to an hour). During timeslot t the energy generated by the power source is denoted as $E_S(t)$. The ETH estimator unit receives in input the amount of energy harvested $E_S(t)$ for all times $t \geq 1$ and outputs N future energy predictions. The prediction intervals are all of equal length L, multiple of T. The overall prediction horizon is $H = NL$. At each timeslot, t predictions about future energy availability $P_S(t, k)$ are computed for the next N prediction intervals as $P_S(t, k) = P_S(t + kL), \quad 0 \leq k \leq N$. The prediction algorithm combines information about the energy harvested during the current time interval with the energy availability obtained in the past. Similar to EWMA, the contribution of older data is exponentially decreasing.

The solution proposed by Noh and Kang [94] is similar to previous approaches. They use the EWMA equation to keep track of the solar energy profile observed in the past. In order to account for short-term varying weather conditions, they introduce a scaling factor φ_n to adjust future energy expectations. This factor is computed as $\varphi_n = x_{n-1}/\mu_{n-1}$, where x_{n-1} is the amount of energy harvested by the end of slot $n - 1$, and μ_{n-1} is the prediction of the amount of energy harvestable during slot $n - 1$ according to the EWMA. Thus, φ_n expresses the ratio between the actual harvested energy at timeslot n and the energy predicted for the same timeslot. This scaling factor is then used to adjust future predictions.

Pro-Energy (*PROfile energy prediction model*, Spenza and Petrioli [95]) is an energy prediction model based on using past energy observations for both solar and wind-based EHWSNs. The main idea of Pro-Energy is to use harvested profiles representing the energy available during different types of "typical" days. For example, days may be classified into sunny, cloudy, or rainy and a characteristic profile may be associated to each of these types. Each day is discretized into a certain number N of timeslots. Predictions are performed once per slot. The energy harvested in the current day is stored in a vector C of length N. A pool of energy profiles observed in the past is also maintained in a $D \times N$ matrix E. These profiles represent the energy obtained during a given number D of typical days. Once per timeslot, Pro-Energy estimates the expected energy availability during the next timeslot by looking at the stored profile that is the most similar to the current day. The similarity of two different profiles is computed as the Euclidean distance between their two vectors, taking into account the first t elements of the vectors, where t is the current timeslot. The value predicted for the next timeslot is then computed based on the value for that slot from the stored profile, possibly scaled by a factor that depends on the current weather conditions.

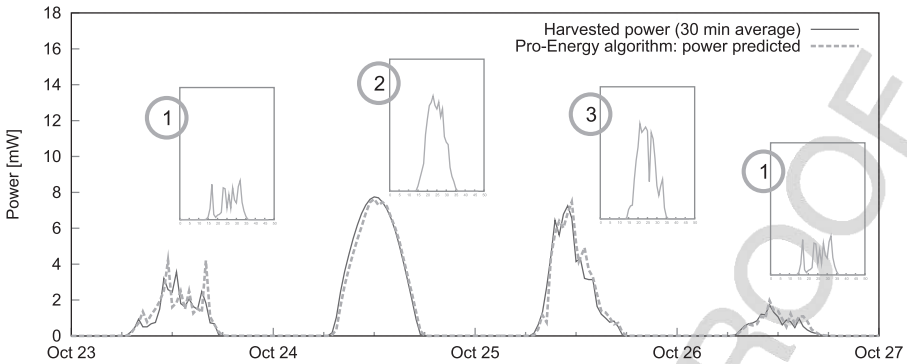

Figure 20.5 Pro-Energy predictions.

Pro-Energy maintains a pool of D typical profiles, each ideally representative of a different weather condition. In order to adapt predictions to changing seasonal patterns, this pool has to be periodically updated. To this aim, at the end of each day, Pro-Energy checks if the current profile—that is, the one just observed—significantly differs from other profiles. If so, an old profile is discarded and the current profile is stored in E. Statistics about profile usage are maintained, so that the profile discarded from the pool is one that has been stored for a long time or that has been used infrequently. Figure 20.5 shows an example of application of the Pro-Energy algorithm over 4 days of solar predictions. During the initial timeslots of October 23rd (day 1), the first stored profile is selected among the typical ones, as it is the most similar to the portion of the current day observed so far. As the day goes on, the shape of the profile changes according to the new observations. Two further different profiles are used for predictions during days 2 and 3. Then, on the fourth day, the first profile is selected again as the most similar to the current observations. Pro-Energy performance compares favorably with respect to previous solutions. For instance, because of the use of energy profiles of typical days, Pro-Energy is able to sensibly decrease prediction errors even in cases with a variable mix of sunny and cloudy days, a case where EWMA instead exhibits poor performance.

We conclude this section by mentioning an approach for energy predictions at medium-length timescales. Sharma et al. [96] explore a system for solar- and wind-powered sensor nodes that derives energy harvesting predictions based on weather forecast. The method is based on the claim that at medium-length timescales (3 hour to 3 days) using weather forecasting data provides greater accuracy than energy predictions based on past observation. The reason they give for the scarce performance of "traditional" predictors is the fact that weather patterns are not consistent in many regions of the United States. They thus formulate a model for solar panels and wind turbines that is able to convert weather forecast data into energy harvesting predictions. The effectiveness of the proposed method is measured by comparing the performance of their solution to that of simple energy predictors based on past observations.

20.5 PROTOCOLS FOR EHWSNs

In this section we describe protocols for EHWSNs, focusing specifically on research areas that have received greater attention, namely, allocation of tasks to the sensors, and MAC and routing solutions.

20.5.1 Task Allocation

Many applications for energy harvesting sensor networks, such as structural health monitoring, disaster recovery, and health monitoring, require real-time reliable network protocols and efficient task scheduling. In such networks, it is important to dynamically schedule node and network tasks based on remaining energy and current energy intake, as well as predictions about future energy availability.

In this section we first provide a classifications of tasks based on their type and characteristics, and then we present an overview of task scheduling algorithms.

Tasks can be categorized as follows:

1. *Periodic vs. Aperiodic*. Depending on their arrival patterns over time, tasks are divided into periodic and aperiodic. Periodic tasks arrive regularly and their inter-arrival time is fixed. Aperiodic tasks, also called on-demand, have arbitrary arrival patterns.
2. *Preemptive vs. Non-preemptive*. A preemptive active task may be preempted at any time, while a non-preemptive task cannot be paused or stopped at any time during its execution.
3. *Dependent vs. Independent*. A task is defined to be independent if its execution does not depend on the running or on the completion of other tasks. A dependent task cannot run until some other tasks have completed their executions.
4. *Multi-version Tasks*. Multi-version tasks have multiple versions, each with different characteristics in terms of time, energy requirements, and priority.
5. *Node vs. Network Tasks*. Each EHWSN node can schedule two kind of tasks: node and network tasks. Tasks that are assigned to, and are executed by, a given node (such as sensing, computing, and communication activities) can be considered node tasks. Tasks that are executed by different nodes (so that a node selection phase has to be performed) or that require the coordination of a group of nodes are considered network tasks. Examples include sensing (in case different sensors are available for executing a given sensing task and task allocation has to be performed at the system level), routing, leader election, cooperative communication, and so on.

Each task is characterized by:

- *Execution Time*. The amount of time during which a task is running on the CPU.
- *Deadline*. The time by which the task should be completed. If the task deadline passes before completing the task, a deadline violation occurs.

- *Power Requirement*. The amount of energy required by a task to be successfully completed. This may include the energy necessary to perform sensing, computation, and communication activities.
- *Reward*. Each task T may be associated with a value or reward r indicating its importance. Rewards can be a function of a task priority [97–100], invocation frequency [101], utility [102], or any other metric. An instance of task i, T_i, contributes r_i units to the total system reward only if it completes by its deadline. The reward (priority) of each tasks may change over time.
- *Running Speed*. The speed of the task currently executing running speed, can be adjusted by employing dynamic voltage and frequency scaling (DVFS) techniques, which lower the operating frequency of the processor (CPU speed) and reduce its energy consumption [97]. As the processor changes its operational frequency and voltage, the task execution speed varies accordingly. Adjusting task speed is desirable because it allows a node to adapt the execution speed of a task based on the energy source availability.

Task scheduling protocols for EHWSNs can be classified depending on the type of tasks they schedule. At the highest level, task scheduling solutions can be divided into protocols that schedule node tasks and protocols that schedule network tasks.

Scheduling Protocols for Node Tasks. The *Lazy Scheduling algorithm* (LSA) [103,104] is one of the earliest work in EHWSN task scheduling. It consider tasks that are aperiodic and preemptive. The execution of tasks is primarily energy driven, in that a task can meet its deadline only if its power requirement is satisfied early enough. As a consequence, the LSA scheduling policy takes into account the property of the energy source, the capacity of the energy storage and the power demands of each single task. LSA introduces the concept of energy variability characterization curves (EVCCs), which capture the dynamics of the energy source. Given a specific energy source, the EVCCs provide guarantees on the produced energy. This concept is used to determine the schedulability of a set of tasks—that is, the determination of the starting times for the execution of each task so that it terminates within its deadline and power requirement. More specifically, the LSA uses an offline schedulability test that, given the EVCCs of the energy source, the capacity of the energy storage, and the maximum power requirement of a running task, determines whether all the deadlines of a given set of tasks can be met or not. LSA suffers from several drawbacks. For instance, in realistic application a task actual energy consumption does not depend on the worst-case energy demand, but rather on factors including the sensor operational state and the circuitry used to perform the task. Furthermore, LSA does not consider dependency among tasks. Finally, the performance of LSA is highly dependent on the accuracy of predicted available energy, which is challenging and, as mentioned, prone to errors.

Audet et al. [105] present two energy-aware techniques, termed *Smooth to Average Method* (STAM) and *Smooth to Full Utilization* (STFU), for scheduling a set of periodic tasks. The aim is to combine the two techniques with known scheduling

algorithms to reduce the likelihood of energy violations while meeting tasks deadlines. STAM and STFU handle energy uncertainty and deadline constraints without relying on any energy prediction model. They consider tasks that are periodic and non-preemptive. The techniques are based on the concept of virtual task. Each real (physical) task has a corresponding virtual task that has the same arrival time, but equal or longer duration. STAM is designed in such a way that the power requirement of a set of tasks is smoothed out to the average power required by all tasks in the set. In particular, given a task set, a corresponding set of virtual tasks is generated where the duration of a virtual task is increased with respect to the duration of its real task if the latter power requirements is greater than average. Virtual tasks are then scheduled (by a know scheduling algorithm, such as Earlier Deadline First) and the real tasks are inserted at the end of their own virtual task timeslot. In so doing, a real task with high power requirement is forced to run after an idle period during which energy is harvested, which decreases the likelihood of energy violation. One possible drawback of STAM is that the execution time of virtual tasks can be so long that no scheduling is possible that meets the deadline of virtual tasks. The STFU technique is proposed to avoid this problem. STFU is similar to STAM; but instead of smoothing out all task power requirements to the average power, it attempts to create a list of virtual tasks that obtain 100% CPU utilization. The goal of STFU is to allocate more time to tasks with higher power requirements, so that a task that required more power has more time to harvest energy before it starts. It is important to note that STAM and STFU are only suitable for offline scheduling, which requires that tasks and their deadlines are known in advance.

The goal of the *multi-version scheduling algorithm* (MVSA) [101] is to execute the most important and valuable periodic tasks while meeting all the timing and energy constraints. Each task is assumed to have multiple versions, each with different characteristics and reward. "Easier" versions of a task execute faster, require less energy, and produce less accurate and valuable results. This static (offline) scheduling solution determines the best task versions and their execution speeds that maximize rewards. Selection is based on worst-case scenario assumptions—that is, the worst-case task execution times, worst-case number of speed changes, minimum harvesting rate, and worst-case battery discharging rates. All this information is assumed to be known in advance. However, a system does not always consume or harvest energy as in the worst case, and oftentime the selection of tasks provided by MVSA is not optimal. To obviate to this problem, the authors propose dynamic algorithms according to which the node periodically checks the current energy storage and accordingly reschedules the tasks.

EL Ghor et al. [106] describe an online scheduling algorithm, called *EDeg* (Earliest Deadline with energy guarantee), that considers tasks that are periodic (fixed task set) and preemptive; and their arrival times, energy demands, and deadlines are known in advance. Tasks are scheduled according to the Earliest Deadline First algorithm. However, before allowing a task to execute, EDeg ensures that the energy available is sufficient to cover the power requirements of all the tasks, considering the replenishment rate of the storage unit. When the stored energy drops below a threshold, EDeg stops the current tasks and starts recharging the battery up to a level that supports task completion. Thus, tasks never run in absence of enough energy. The requirement to

know in advance the arrival times, the deadlines, and the energy demands of the tasks seriously limits the applicability of this algorithm in real-life application scenarios.

Steck and Rosing [102] present a *task utility scheduling* protocol with two main goals: First, given a certain level of utility, determine the expected execution time and energy consumption of a set of tasks. Second, given a time constraint, find the maximum achievable utility for the set of tasks. This algorithm schedules the tasks by balancing task utility and execution time subject to an energy constraint aimed to ensure the energy neutrality of the system. The relationship among the tasks is assumed to be known and modeled by a directed acyclic graph (DAG). In addition, the task execution times, past energy harvesting information, tasks qualities, and utility relationships, are given in advance. For most applications, the utility is modeled as accuracy and as a function of the task priorities. A task with higher priority is executed with higher utility.

In reference 107, an energy-aware DVFS (EA-DVFS) scheduling algorithm is proposed that dynamically matches its schedules to the stored energy and harvestable energy in the future. Specifically, tasks are executed at full speed if the stored energy is sufficient. Execution speed is slowed down when the stored energy is not sufficient. This work has been extended further in [98] by the adaptive scheduling and DVFS algorithm (AS-DVFS). AS-DVFS adaptively tunes the operation voltage and frequency of a node processor whenever possible while maintaining the time and energy constraints. The goal of AS-DVFS is to reach a system-wide energy efficiency by scheduling and running the tasks at the lowest possible speed and allocating the workload to the processor as evenly as possible. Moreover, it decouples the timing and energy constraints, addressing them separately. A harvesting-aware DVFS (HA-DVFS) algorithm is proposed in [97] to further improve the system performance and energy efficiency of EA-DVFS and AS-DVFS. In particular, the main goals of HA-DVFS are to keep the running speed of the tasks always at the lowest possible value and avoid wasting harvested energy. Based on the prediction of the energy harvesting rate in the near future, HA-DVFS schedules the tasks and tunes the speed and workload of the system to avoid energy overflow. Three different time series prediction techniques, namely regression analysis, moving average, and exponential smoothing, are used for predicting the harvested energy. Similar to AS-DVFS, HA-DVFS decouples the energy constraints and timing constraints to reduce the complexity of scheduling algorithm.

Another *DVFS-based task scheduling* algorithm is presented in reference 99. The new task scheduler is based on a linear regression model embedded into the DVFS functionality. The model is used to correlate the number of tasks and their complexity with their execution time, energy consumption, and data accuracy. The main objectives of the proposed scheduler are maximizing system performance given the current energy availability, increasing the efficiency of energy utilization, and improving task accuracy. The scheduler effectiveness is demonstrated through an application to structural health monitoring. The authors argue that this type of application (as well as health-care applications) is particularly best served by the new scheduler since the tasks they generate are mostly periodic tasks instead of sporadic externally triggered events, which makes linear regression particularly effective.

Scheduling Protocols for Network Tasks. Task allocation at the network level concerns matching the resources of a WSN to appropriate tasks (missions), which may come to the network dynamically. This is a nontrivial task, because a given node may offer support to different missions with different levels of accuracy and fit (*utility*). Missions may vary in importance (*profit*) and amount of resources they require (*demand*). They may also appear in the network at any time and may have different duration. The goal of a sensor-missions assignment algorithm is to assign available nodes to appropriate missions, maximizing the profit received by the network for mission execution. Although solutions for WSNs with battery-operated nodes have been proposed for this problem [108–111], until recently [112] no attention has been given to networks whose nodes have energy harvesting capabilities. For these networks, new paradigms for mission assignments are needed, which take into account that nodes currently having little or no energy left might have enough in the future to carry out new missions. These solutions should also consider that energy availability is time-dependent and that energy storage is limited in size and time (due to leakage) so that energy usage should be carefully planned to minimize waste of energy.

EN-MASSE [112] is a decentralized heuristic for sensor-mission assignment in energy-harvesting wireless sensor networks, which effectively takes into account the characteristics of an energy harvesting system to decide which node should be assigned to a particular mission at a given time. It is able to handle hybrid storage systems consisting of multiple energy storage devices (super-capacitor and battery) and to adapt its behavior according to the current and expected energy availability of the node while maximizing the efficient usage of the energy harvested. EN-MASSE has been designed for sensing task assignment. Each mission arrives in the network at a specific geographic location l_i. In EN-MASSE the sensor node closest to l_i is selected as the *mission leader* and coordinates the process of assigning nodes to the mission. The communication protocol described in references 109 and 110 is selected for exchanging information between the mission leader and the nearby nodes. Each time a new mission arrives in the network, the leader advertises mission information, including mission location, profit, and demand, to its two-hop neighbors, starting the *bidding phase* for the mission. During this bidding phase, each node receiving the mission advertisement message sent by the leader will autonomously decide whether to bid for participating to the mission or not. Such a decision is taken accordingly to the bidding scheme used by the node. Specifically, nodes classify incoming missions into four different classes: free, recoverable, capacitor-sustainable, and battery required. This classification is made according to the impact that executing a mission of a given class would have on the energy reservoir of the node. *Free* missions are those that can be executed by the node "for free," because they arrive when the node super-capacitor is full and their energy cost is expected to be fully sustained by the energy harvested during their duration. Ideally, executing a mission of this class should not affect the energy reservoir of the node at all. *Recoverable* missions are those whose energy cost can be sustained using the energy stored in the super-capacitor and whose energy cost can be recovered through harvesting in a small period of time. This time is set as the missions interarrival time, so that choosing to execute a recoverable mission is not likely to affect the node capability of bidding on the next one. *Capacitor-sustainable*

missions occur if the total energy cost of the mission can be sustained using only the super-capacitor. This cost is not expected to be recovered through harvesting before the arrival of the next mission. *Battery-required* missions are those whose energy cost must be totally or partially supplied by the battery. The EN-MASSE bidding scheme gives higher priority to missions that would have less impact on energy reservoir of the node. Thus, nodes always accept to execute free missions. EN-MASSE makes bidding decisions also taking into account the importance and the utility of the missions. These two factors remaining equal, nodes implement a more aggressive bidding policy for recoverable missions than for capacitor-sustainable ones. The most conservative bidding policy is used for battery-required missions. Since the energy stored in the battery is limited and nonreplenishable, nodes choose to use precious battery energy only to execute the most critical missions. EN-MASSE uses an energy prediction model to estimate the energy a node will receive from the ambient source and to classify missions. Different predictors, such as the ones described in Section 20.4, may be used in combination with EN-MASSE.

20.5.2 Harvesting-Aware Communication Protocols: MAC and Routing

Harvesting capabilities have changed the design objectives of communication protocols for EHWSNs from energy conservation to opportunistic optimization of the use of the harvested energy. This fundamental change calls for novel communication protocols. The aim of this section is to explore the solutions proposed so far for EHWSN medium access control (MAC) and routing.

MAC Protocols. We describe exemplary MAC protocols for EHWSNs, which include ODMAC [113], EA-MAC [114,115], MTTP [116], and PP-MAC [117].

ODMAC [113] is an on-demand MAC protocol for EHWSNs. It is based on three basic ideas: minimizing wasting energy by moving the idle listening time from the receiver to the transmitter; adapting the duty cycle of the node to operate in the energy neutral operation (ENO) state, and reducing the end-to-end delay by employing an opportunistic forwarding scheme. In ODMAC, transmission scheduling is accomplished by having available receivers broadcasting a beacon packet periodically. Nodes wishing to transmit listen to the channel, waiting for a beacon. Upon receiving a beacon, the transmitter attempts packet transmission to the source of the beacon. Setting the beacon period imposes a tradeoff between energy consumption and end-to-end latency: When the beacon period is short, more energy is consumed for transmitting beacons. Longer beacon periods result in higher energy conservation. Figure 20.6 shows the operation mechanism of the ODMAC protocol. ODMAC supports a dynamic duty cycle mode, in which the sensing period and the beacon periods of each node is periodically adjusted according to the current power harvesting rate. To this end, a battery level threshold is selected and periodically compared the current battery level to determine if the duty cycle should be increased or decreased. ODMAC also includes the concept of opportunistic forwarding, in which, instead of waiting for a specific beacon, each frame is forwarded to the sender of the first beacon received as long as it is included in a list of potential forwarders. In ODMAC it is assumed that

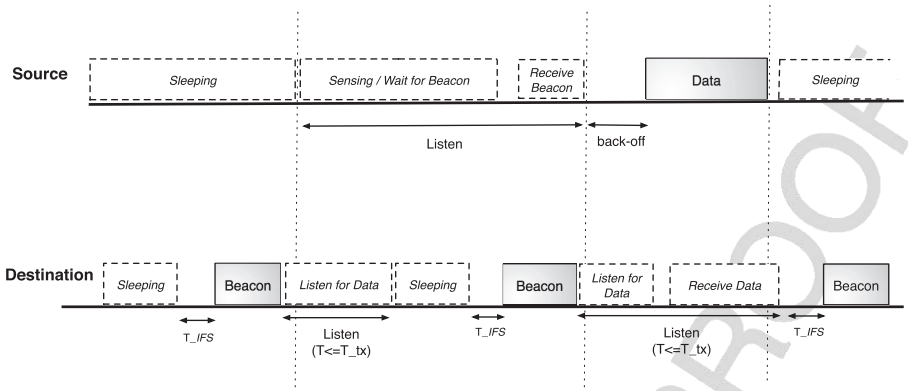

Figure 20.6 ODMAC: data packet transmission.

charging (harvesting) is independent of sensor node operations and thus a sensor can harvest available energy during all operational states—that is, irrespective of whether it is sleeping, listening, transmitting, and so on. ODMAC is not suitable to be used in lossy environment, as it does not acknowledge and retransmits packets.

EA-MAC [114,115] is a MAC protocol proposed for EHWSNs with RF energy transfer. EA-MAC uses the node energy harvesting status as a control variable to tune the node duty cycles and backoff times. To this end, two adaptive methods, energy adaptive duty cycle and energy adaptive contention algorithm, are proposed to manage the node duty cycle and backoff time depending on the harvested power rate. EA-MAC is similar to the unslotted CSMA/CA algorithm in IEEE 802.15.4 [118], but its sleep duration, backoff times, and state transitions are controlled by the average amount of harvestable energy. When a node harvested energy level is equal to the energy required to transmit a packet, the node transitions from sleep state to active state. Then it follows a CSMA/CA scheme to transmit the packet. If the channel is idle during the clear channel assessment (CCA) period, the node transmits a data packet. If the channel is busy, the node decides to either perform the random backoff procedure or terminate the CSMA/CA algorithm. The number of backoff slots depends on the current energy harvesting rate. Analytical models for the throughput and fairness of EA-MAC are provided and validated by simulations [115]. Similar to ODMAC, EA-MAC assumes the sensor node can harvest energy in any operational states. EA-MAC does not consider some important application requirements, such as end-to-end delay, and provides no mechanism to optimize network performance and lifetime. In addition, EA-MAC suffers from the hidden terminal problem, which results in increased collisions. Finally, its performance is not compared to any other protocol, such as slotted or unslotted CSMA/CA.

The *Probabilistic polling* (PP-MAC) protocol [117] is a polling-based MAC mechanism that leverages the energy characteristics of EHWSNs to enhance the performance of traditional polling schemes in terms of throughput, fairness, and scalability. PP-MAC is similar to the polling protocol described in reference 119: The sink

broadcasts a polling packet and the polled sensor responds with a packet transmission (single-hop topology). Instead of carrying the ID of a specific sensor, the polling packet contains a contention probability that the receiving sensor nodes use to decide whether to transmit their packet or not. The contention probability is computed based on current energy harvesting rate, number of nodes, and packet collisions. The probabilistic polling protocol increases the contention probability gradually when no sensor responds to the polling packet. It decreases it whenever there is a collision between two or more sensor nodes. As a result, and based on an additive-increase multiplicative-decrease (AIMD) mechanism, the contention probability is decreased when more nodes are added to the EHWSN, and increased when nodes fail or are removed from the network. Moreover, in case of increase/decrease of the average energy harvesting rates, the contention probability is decreased/increased accordingly. PP-MAC uses the charge-and-spend harvesting strategy in which it first accumulates enough energy and then goes to the receive state to listen and receive the polling packet. Nodes return back to charging state either when their energy falls below the energy required to transmit a data packet or after transmitting their packet. Energy is assumed to be harvested only while in charging state. Analytical formulas and analysis of the throughput performance of PP-MAC is presented and validated by simulations. PP-MAC does not support multihop EHWSNs.

The *multi-tier probabilistic polling* (MTPP) protocol [116] extends probabilistic polling à la PP-MAC to multihop data delivery in EHWSNs with no energy storage—that is, whose operations are powered solely by energy currently harvested (charge-and-spend harvesting policy). The polling packets generated by the sink are sent to the immediate neighbors of the sink, and these nodes forward them to nodes in following tiers, in a "wave-expanding" fashion (Figure 20.7). Polling packets and data packets are broadcast and relayed, respectively, from tier to tier until they reach their destination. As the number of tiers increases, the overhead of polling packets and packet collisions also increase, imposing higher latencies. Analytical models for energy consumption, energy harvesting, energy storage, and interference as well as

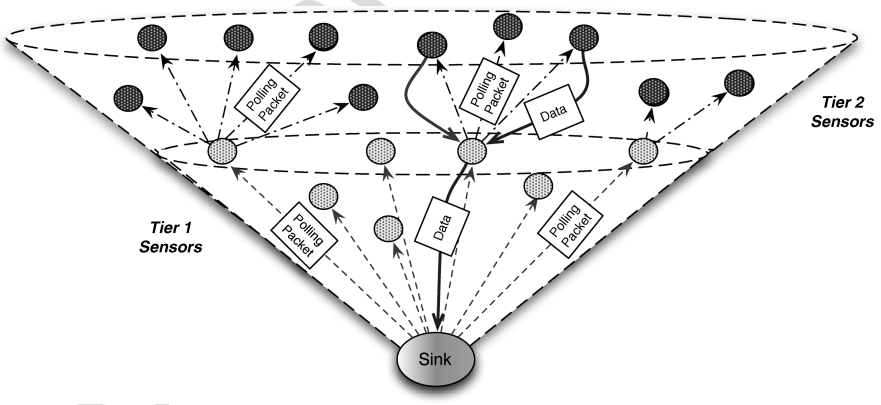

Figure 20.7 Overview of MTTP multi-tier EHWSN architecture.

Table 20.2 Comparison of MAC Protocols for EHWSNs

	ODMAC	EA-MAC	PP-MAC	MTTP
Topology	Multihop	Single-hop	Single-hop	Multihop
Harvesting policy	Store	Store	Charge-and-spend	Charge-and-spend
Harvesting technology	Generic	RF energy transfer	Solar	Solar
Latency	Increases with traffic	Fair	Low	High
Channel access type	CSMA/CA	CSMA/CA	Polling	Polling
Scalability	Good	Weak	Good	Good
Communication patterns	All	Convergecast	Convergecast	Convergecast & Broadcast
Performance evaluation	OPNET simulations	OPNET simulations	Real measurements & QualNet	Real testbed
Use of control packets	Yes	No	Yes	Yes
Adaptivity to changes	Fair	Good	Good	Good

the delivery probability are presented in reference 120 and validated by numerical analysis.

A comparative summary of the characteristics of these presented MAC protocol is presented in Table 20.2.

Routing Protocols. Energy-efficient routing has been widely explored for battery operated WSNs [121–126]. EHWSNs exhibit unique characteristics and among their man objective there is not only extending the network lifetime, but also the maximization of the workload that the network can sustain, given the source-dependent energy availability of the nodes [127]. This is the rationale behind protocols for routing in EHWSNs that we present in this section.

HESS. Pais et al. [128] propose a routing protocol termed HESS for *hybrid energy storage systems* combining a super-capacitor with a rechargeable battery. Their approach is to favor routes that use more energy from super-capacitors and that go through nodes with higher harvesting rates. Their work stems from the fact that a rechargeable battery can only sustain a limited amount of recharge cycles before its capacity falls below 80% of its original capacity. The authors propose a cost–benefit function that reflects the cost and revenue of choosing a specific node as a relay for a packet. Such a function considers several factors, including the relay hop count, its residual battery and super-capacitor energy, the energy it harvested previously, the remaining cycles of its battery, and its queue occupancy. Nodes with higher residual energy, harvesting rate, and remaining battery cycles are preferred as relays, while

choosing nodes with higher hop count or lower transmission queue availability is less desirable. These cost/benefit factors are combined together, opportunely weighted, in order to account for both desirable and undesirable parameters. The overall goal of HESS is to minimize the cost of each end-to-end transmission. A simulation-based performance evaluation shows that HESS provides an average 10% increase of network residual energy with respect to the Energy Aware Routing (EAR) protocol [129], without compromising the data packet delivery ratio.

DEHAR (Distributed Energy Harvesting Aware Routing Algorithm [130]) is an adaptive and distributed routing for EHWSNs that calculates the shortest paths to the sink based on hop count and the energy availability of the nodes. To add energy-harvesting awareness to the algorithm, a local penalty is assigned to each node. This penalty, dynamically updated, is inversely proportional to the fraction of energy available to the node. When the energy buffer of the node is fully charged, this penalty should ideally be zero, while it should tend to infinity when the node has depleted its energy. When a change in the local penalty of a node occurs, it advertises it to its immediate neighbors. For each node, the local penalty is combined with distance from the sink to define the node energy distance, which is used by other nodes when choosing a potential relay. The energy distance of a node may become a local minimum if the penalty of a node neighbor is changed due to variations in its energy availability. To solve this problem, distributed penalties are introduced. Each time a node receives an energy update from a neighbor, it checks if it has become a local minimum. If this is the case, it increases its distributed distance penalty and advertises it to its immediate neighbors. Distributed and local penalty of a node are finally merged in a total penalty that is distributed to neighbor nodes.

EHOR: Energy Harvesting Opportunistic Routing (Eu et al. [131]) is an opportunistic routing protocol for EHWSNs powered solely by energy harvesters (no batteries). Nodes of EHWSNs powered only by harvested energy are normally awake for a short period of time, and then they shut down to recharge. To determine the best active relays in its neighborhood, a node partitions potential relays in groups, or regions, based on their distance from the sink and on the residual energy of the nodes in the region. After receiving a data packet, the potential relay that is the closest to the sink rebroadcasts it. Each node in the network follows a charging cycle consisting of (a) a charging phase, during which the power consumption is minimal and the node waits to be recharged by the harvested energy, (b) a receive phase, to which the node switches when it is fully charged, and (c) an optional transmit phase. Simulation results show that EHOR achieves good performance and outperforms traditional opportunistic routing protocols. EHOR, however, assumes that the network topology is linear—that is, that nodes are uniformly deployed over a given interval and does not work in 2D topologies.

Noh and Yoon [132] introduce *D-APOLLO* (Duty-cycle-based Adaptive toPOLogical KR aLgOrithm) a harvesting-aware geographic routing protocol. Their approach aims at maximizing the utilization of the harvested energy and reducing latency by dynamically and periodically adapt the duty-cycle and the knowledge range (KR) of each node. The knowledge range of each node is the topological extent of the information that it collects. Dimensioning the KR involves a tradeoff between the optimality

of the path produced by the routing algorithm and the energy needed to collect and maintain a larger quantity of information about a node neighbors. The duty cycle of the nodes and their knowledge range are usually fixed in battery-operated WSNs. D-APOLLO, instead, periodically tries to find the duty cycle and the knowledge range that maximize utilization of the harvested energy based on the expected harvesting power rate, the residual energy of the node, and the predicted energy consumption.

The *Energy-opportunistic Weighted Minimum Energy* (E-WME, Lin et al. [133]) calculates the shortest path to the sink based on a cost function metric that considers the residual energy of the node, its battery capacity, its harvesting power rate, and the energy required for receiving and transmitting packets. The cost of each node is an exponential function of the nodal residual energy, a linear function of the transmit and receive energies, and an inversely linear function of the harvesting power rate. The authors show that as an online protocol E-WME has an asymptotically optimal competitive ratio and that it can lead in practice to significant improvements in the performance of EHWSNs with respect to other harvesting-unaware routing protocols.

Bogliolo et al. [134] present a modified version of the Ford–Fulkerson algorithm to determine the maximum energetically sustainable workload of an EHWSN. Their *Randomized Max-Flow* (R-MF) protocol, along with its enhancement *Randomized Minimum Path Recovery Time* (R-MPRT) [127], selects the edge over which to route the packet with probability proportional to the maximum flow through that edge. More specifically, in R-MF and R-MPRT the cost $C_{u,v}$ of routing a packet through a link (u, v) is expressed as

$$C_{u,v} = \frac{p_u}{e^{u,v}_{\text{routing}}} \tag{20.1}$$

where p_u is the harvesting power rate of node u, and $e^{u,v}_{\text{routing}}$ is the energy needed to process or generate a packet at node u and to transmit it to node v through the link (u, v).

Hasenfratz et al. [135] analyze and compare three state-of-the-art routing protocols for EHWSNs: R-MF, E-WME, and R-MPRT. In their work, they show the influence of various real-life settings on their performance, namely, (1) the usage of a low-power MAC protocol instead of an ideal one, (2) the effect of considering a realistic wireless channel, and (3) the influence of the protocol overhead. They also propose a modified version of the R-MPRT algorithm, which is able to outperform R-MPRT in scenarios where little energy is harvested from the environment. More precisely, they suggest to modify equation (20.1) as follows:

$$C_{u,v} = \frac{E_u}{e^{u,v}_{\text{routing}}} \tag{20.2}$$

where E_u is the amount of energy available at node u, and $e^{u,v}_{\text{routing}}$ is the energy needed to process or generate a packet at node u and transmit it to node v through the link (u, v).

Zeng et al. [136] propose two geographic routing algorithms, called GREES-L and GREES-M, which take into account energy harvesting conditions and link

quality. Each node is required to maintain its one-hop neighbor information including the neighbors location, residual energy, energy harvesting rate, energy consuming rate, and wireless link quality. While forwarding a packet toward its destination, the nodes in the network try to balance the energy consumption across their neighbors, by minimizing a cost function combining the information they maintain. Such cost function is defined based on two factors, namely, the geographical advance per packet transmission and the energy availability of the receiving node. The difference between GREES-L and GREES-M is in the way they combine the two factors: GREES-L uses a linear combination of them, while GREES-M multiplies them. GREES-L and GREES-M only consider as potential relay neighbor nodes that provide positive advancement towards the sink, which is typical of greedy geographic forwarding. GREES-L and GREES-M have been shown to be more energy efficient than the corresponding residual-energy-based protocols via simulations.

Doost et al. [137] propose a new routing metric based on the charging ability of the sensor nodes. The metric can be used along existing routing protocols for wireless ad hoc and sensor networks. In the paper, it is demonstrated over the well-know ad hoc routing protocol AODV [138] on EHWSNs powered by wireless energy transfer. Routes are formed with nodes that have the best energy charging characteristics. In particular, each node selects the path with the lowest value of the maximum charging times. Simulation results show that this choice is effective in producing high network lifetime and throughput.

ACKNOWLEDGMENTS

This work was supported in part by the NSF award "GENIUS: Green sEnsor Networks for aIr qUality Support" (NSF CNS 1143681) and by the EU funded project STREP FP7 "GENESI: Green sEnsor NEtworks for Structural MonItoring" (grant agreement n. 257916). Dora Spenza is a recipient of the Google Europe Fellowship in Wireless Networking, and this research is supported in part by this Google Fellowship.

REFERENCES

1. I. F. Akyildiz and M. C. Vuran. *Wireless Sensor Networks*. Advanced Texts in Communications and Networking. John Wiley & Sons, Hoboken, NJ, 2010.
2. Moteiv Corporation. Datasheet Telos Rev B (Low Power Wireless Sensor Module), May 2004.
3. Crossbow Technology, Inc. Datasheet MICAz, 2004.
4. U. M. Colesanti, S. Santini, and A. Vitaletti. DISSsense: An adaptive ultralow-power communication protocol for wireless sensor networks. In *Proceedings of IEEE DCOSS 2011*, June 2011, pp. 1–10.
5. I. Buchmann. *Batteries in a Portable World: A Handbook on Rechargeable Batteries for Non-engineers*, 2nd ed. Cadex Electronics, Inc., Richmond, BC, Canada, 2001.

6. T. B. Reddy and D. Linden, Eds. *Linden's Handbook of Batteries*, 4th ed. McGraw Hill, New York, 2010.
7. S. Sudevalayam and P. Kulkarni. Energy harvesting sensor nodes: Survey and implications. *IEEE Communications Surveys Tutorials* **13**(3):443–461, 2011.
8. T. Zhu, Z. Zhong, Y. Gu, T. He, and Z.-L. Zhang. Leakage-aware energy synchronization for wireless sensor networks. In *Proceedings of ACM MobiSys 2009*, New York, 2009, pp. 319–332.
9. D. Brunelli. Miniaturized solar scavengers for ultra-low power wireless sensor nodes. In *Proceedings of WEWSN 2008*, Santorini Island, Greece, June 2008.
10. F. Simjee and P. H. Chou. Everlast: Long-life, supercapacitor-operated wireless sensor node. In *Proceedings of ISLPED 2006*, Tagernsee, Germany, October 4–6, 2006, pp. 197–202.
11. P. Dutta, J. Hui, J. Jeong, S. Kim, C. Sharp, J. Taneja, G. Tolle, K. Whitehouse, and D. Culler. Trio: Enabling sustainable and scalable outdoor wireless sensor network deployments. In *Proceedings of ACM/IEEE IPSN 2006*, Nashville, TN, April 19–21, 2006, pp. 407–415.
12. X. Jiang, J. Polastre, and D. Culler. Perpetual environmentally powered sensor networks. *Proceedings of ACM/IEEE IPSN 2005*, April 25–27, 2005, pp. 463–468.
13. C. Park and P. H. Chou. AmbiMax: Autonomous energy harvesting platform for multi-supply wireless sensor nodes. In *Proceedings of IEEE SECON 2006*, Reston, VA, September 25–28, 2006, pp. 168–177.
14. P. Corke, T. Wark, P. Valencia, and P. Sikka. Long-duration solar-powered wireless sensor networks. In *Proceedings of EmNets 2007*, Cork, Ireland, June 25–26, 2007, pp. 33–37.
15. C. Park and P. H. Chou. Power utility maximization for multiple-supply systems by a load-matching switch. In *Proceedings of ISLPED 2004*, August 9–11, 2004, pp. 168–173.
16. V. Raghunathan, A. Kansal, J. Hsu, J. Friedman, and M. B. Srivastava. Design considerations for solar energy harvesting wireless embedded systems. In *Proceedings of ACM/IEEE IPSN 2005*, Los Angeles, April 25–27, 2005, pp. 457–462.
17. J. Kowal, E. Avaroglu, F. Chamekh, A. Senfelds, T. Thien, D. Wijaya, and D. U. Sauer. Detailed analysis of the self-discharge of supercapacitors. *Journal of Power Sources* **196**(1):573–579, 2011.
18. G. V. Merrett, A. S. Weddell, A. P. Lewis, N. R. Harris, B. M. Al-Hashimi, and N. M. White. An empirical energy model for super-capacitor powered wireless sensor nodes. In *Proceedings of IEEE ICCCN 2008*, St. Thomas, US Virgin Islands, August 3–7, 2008, pp. 1–6.
19. A. Kansal, J. Hsu, S. Zahedi, and M. B. Srivastava. Power management in energy harvesting sensor networks. *ACM Transactions in Embedded Computing Systems* **6**(4):Article 32, 2007.
20. C. Renner, J. Jessen, and V. Turau. Lifetime prediction for supercapacitor-powered wireless sensor nodes. In *Proceedings of FGSN 2009*, Hamburg, Germany, August 13–14, 2009, pp. 55–58.
21. C. F. Chiasserini and R. R. Rao. Pulsed battery discharge in communication devices. In *Proceedings of ACM/IEEE MobiCom 1999*, Seattle, WA, August 15–20, 1999, pp. 88–95.
22. R. Rao, S. Vrudhula, and D. N. Rakhmatov. Battery modeling for energy aware system design. *Computer Magazine* **36**(12):77–87, 2003.

23. M. Doyle, T. F. Fuller, and J. Newman. Modeling of galvanostatic charge and discharge of the lithium/polymer/insertion cell. *Journal of the Electrochemical Society* **140**(6): 1526–1533, 1993.
24. T. F. Fuller, M. Doyle, and J. Newman. Simulation and optimization of the dual lithium ion insertion cell. *Journal of the Electrochemical Society* **141**(1):1–10, 1994.
25. M. Pedram. Design considerations for battery-powered electronics. In *Proceedings of Design Automation Conference*, New Orleans, LA, June 21–25, 1999, pp. 861–866.
26. K. C. Syracuse and W. D. K. Clark. A statistical approach to domain performance modeling for oxyhalide primary lithium batteries. In *Proceedings of the* 12*th Annual Battery Conference on Applications and Advances*, Long Beach, CA, January 14–17, 1997, pp. 163–170.
27. C. F. Chiasserini and R. R. Rao. Energy efficient battery management. *IEEE Journal on Selected Areas in Communications* **19**(7):1235–1245, 2001.
28. H. J. Bergveld, W. S. Kruijt, and P. H. L. Notten. Electronic-network modeling of rechargeable NiCd cells and its application to the design of battery management systems. *Journal of Power Sources* **77**(2):143–158, 1999.
29. S. Gold. A PSPICE macromodel for lithium-ion batteries. In *Proceedings of the* 12*th Annual Battery Conference on Applications and Advances*, Long Beach, CA, January 14–17, 1997, pp. 215–222.
30. L. Benini, G. Castelli, A. Macii, E. Macii, M. Poncino, and R. Scarsi. A discrete-time battery model for high-level power estimation. In *Proceedings of DATE 2000*, Paris, France, March 27–30, 2000, pp. 35–41.
31. D. N. Rakhmatov and S. B. K. Vrudhula. An analytical high-level battery model for use in energy management of portable electronic systems. In *Proceedings of IEEE/ACM ICCAD 2001*, San Jose, CA, November 4–8, 2001, pp. 488–493.
32. P. D. Mitcheson, E. M. Yeatman, G. K. Rao, A. S. Holmes, and T. C. Green. Energy harvesting from human and machine motion for wireless electronic devices. *Proceedings of the IEEE* **96**(9):1457–1486, September 2008.
33. E. O. Torres. *An Electrostatic CMOS/BiCMOS Li Ion Vibration-Based Harvester-Charger IC*. PhD thesis, Georgia Institute of Technology, May 2010.
34. E. O. Torres and G. A. Rincón-Mora. Long-lasting, self-sustaining, and energy-harvesting system-in-package (SiP) wireless micro-sensor solution. In *Proceedings of INCEED 2005*, Charlotte, NC, July 24–30 2005.
35. F. Yildiz. Potential ambient energy-harvesting sources and techniques. *The Journal of Technology Studies* **35**(1):40–48, 2009.
36. S. Chalasani and J. M. Conrad. A survey of energy harvesting sources for embedded systems. In *Proceedings of the IEEE Southeastcon 2008*, April 2008, pp. 442–447.
37. S. Roundy, P. K. Wright, and J. Rabaey. A study of low level vibrations as a power source for wireless sensor nodes. *Computer Communications* **26**(11):1131–1144, 2003.
38. V. R. Challa, M. G. Prasad, and F. T. Fisher. Towards an autonomous self-tuning vibration energy harvesting device for wireless sensor network applications. *Journal of Smart Materials and Structures* **20**(2):1–11, 2011.
39. Y. Chen, D. Vasic, F. Costa, W. Wu, and C. K. Lee. Self-powered piezoelectric energy harvesting device using velocity control synchronized switching technique. In *Proceedings of IEEE IECON 2010*, Phoenix, AZ, November 7–10, 2010, pp. 1785–1790.

40. J. G. Rocha, L. M. Goncalves, P. F. Rocha, M. P. Silva, and S. Lanceros-Mendez. Energy harvesting from piezoelectric materials fully integrated in footwear. *IEEE Transactions on Industrial Electronics* **57**(3):813–819, 2010.
41. Y. Suzuki and S. Kawasaki. An autonomous wireless sensor powered by vibration-driven energy harvesting in a microwave wireless power transmission system. In *Proceedings of EUCAP 2011*, Roma, Italy, April 11–15, 2011, pp. 3897–3900.
42. M. Zhu and E. Worthington. Design and testing of piezoelectric energy harvesting devices for generation of higher electric power for wireless sensor networks. In *Proceedings of the IEEE Sensors*, Christchurch, New Zealand, October 25–28, 2009, pp. 699–702.
43. R. Moghe, Y. Yang, F. Lambert, and D. Divan. A scoping study of electric and magnetic field energy harvesting for wireless sensor networks in power system applications. In *Proceedings of IEEE ECCE 2009*, San Jose, CA, September 20–24, 2009, pp. 3550–3557.
44. S. J. Roundy. *Energy Scavenging for Wireless Sensor Nodes with a Focus on Vibration to Electricity Conversion*. PhD thesis, University of California at Berkeley, Berkeley, CA, May 2003.
45. M. K. Stojcev, M. R. Kosanovic, and L. R. Golubovic. Power management and energy harvesting techniques for wireless sensor nodes. In *Proceedings of TELSIKS 2009*, Niš, Serbia, October 7–9, 2009, pp. 65–72.
46. C. He, A. Arora, M. E. Kiziroglou, D. C. Yates, D. O'Hare, and E. M. Yeatman. MEMS energy harvesting powered wireless biometric sensor. In *Proceedings of BSN 2009*, Berkeley, CA, June 3–5, 2009, pp. 207–212.
47. M. E. Kiziroglou, C. He, and E. M. Yeatman. Flexible substrate electrostatic energy harvester. *IEEE Electronics Letters* **46**(2):166–167, 2010.
48. J. C. Park, D. H. Bang, and J. Y. Park. Micro-fabricated electromagnetic power generator to scavenge low ambient vibration. *IEEE Transactions on Magnetics* **46**(6):1937–1942, 2010.
49. O. Zorlu, E. T. Topal, and H. Küandlah. A vibration-based electromagnetic energy harvester using mechanical frequency up-conversion method. *IEEE Sensors Journal* **11**(2):481–488, 2011.
50. S. Ayazian, E. Soenen, and A. Hassibi. A photovoltaic-driven and energy-autonomous CMOS implantable sensor. In *Proceedings of IEEE VLSIC 2011*, June 2011, pp. 148–149.
51. M. Barnes, C. Conway, J. Mathews, and D. K. Arvind. ENS: An energy harvesting wireless sensor network platform. In *Proceedings of ICSNC 2010*, August 2010, pp. 83–87.
52. C. Chen and P. H. Chou. DuraCap: A supercapacitor-based, power-bootstrapping, maximum power point tracking energy-harvesting system. In *Proceedings of ISLPED 2010*, August 2010, pp. 313–318.
53. Y. Chen, Q. Wang, J. Gupchup, and A. Terzis. Tempo: An energy harvesting mote resilient to power outages. In *Proceedings of IEEE LCN 2010*, October 2010, pp. 933–934.
54. P. Sitka, P. Corke, L. Overs, P. Valencia, and T. Wark. Fleck—A platform for real-world outdoor sensor networks. In *Proceedings of ISSNIP 2007*, December 2007, pp. 709–714.
55. V. Kyriatzis, N. S. Samaras, P. Stavroulakis, H. Takruri-Rizk, and S. Tzortzios. Enviromote: A new solar-harvesting platform prototype for wireless sensor networks. In *Proceedings of IEEE PIMRC 2007*, September 2007, pp. 1–5.

56. M. Minami, T. Morito, H. Morikawa, and T. Aoyama. Solar Biscuit: A battery-less wireless sensor network system for environmental monitoring applications. In *Proceedings of INSS 2005*, June 2005, pp. 1–6.
57. N. S. Hudak and G. G. Amatucci. Small-scale energy harvesting through thermoelectric, vibration, and radio frequency power conversion. *Journal of Applied Physics* **103**(10): 1–24, 2008.
58. J. G. Webster. *The Measurement, Instrumentation, and Sensors Handbook*. The electrical engineering handbook series. CRC Press, Boca Raton, FL, 1998.
59. R. Abbaspour. A practical approach to powering wireless sensor nodes by harvesting energy from heat flow in room temperature. In *Proceedings of IEEE ICUMT 2010*, October 2010, pp. 178–181.
60. X. Lu and S.-H. Yang. Thermal energy harvesting for WSNs. In *Proceedings of IEEE SMC 2010*, October 2010, pp. 3045–3052.
61. R. Heer, J. Wissenwasser, M. Milnera, L. Farmer, C. Höpfner, and M. Vellekoop. Wireless powered electronic sensors for biological applications. In *Proceedings of IEEE EMBC 2010*, September 4, 2010, pp. 700–703.
62. S. Mandal, L. Turicchia, and R. Sarpeshkar. A low-power, battery-free tag for body sensor networks. *IEEE Pervasive Computing* **9**(1):71–77, 2010.
63. H. Reinisch, S. Gruber, H. Unterassinger, M. Wiessflecker, G. Hofer, W. Pribyl, and G. Holweg. An electro-magnetic energy harvesting system with 190 nW idle mode power consumption for a BAW based wireless sensor node. *IEEE Journal of Solid-State Circuits* **46**(7):1728–1741, 2011.
64. F. Fei, J. D. Mai, and W. J. Li. A wind-flutter energy converter for powering wireless sensors. *Sensors and Actuators A: Physical* **173**(1):163–171, 2012.
65. S. P. Matova, R. Elfrink, R. J. M. Vullers, and R. van Schaijk. Harvesting energy from airflow with a michromachined piezoelectric harvester inside a Helmholtz resonator. *Journal of Micromechanics and Microengineering* **21**(10):1–6, 2011.
66. E. Sardini and M. Serpelloni. Self-powered wireless sensor for air temperature and velocity measurements with energy harvesting capability. *IEEE Transactions on Instrumentation and Measurement* **60**(5):1838–1844, 2011.
67. Y. K. Tan and S. K. Panda. Energy harvesting from hybrid indoor ambient light and thermal energy sources for enhanced performance of wireless sensor nodes. *IEEE Transactions on Industrial Electronics* **58**(9):4424–4435, 2011.
68. Y. K. Tan and S. K. Panda. Self-autonomous wireless sensor nodes with wind energy harvesting for remote sensing of wind-driven wildfire spread. *IEEE Transactions on Instrumentation and Measurement* **60**(4):1367–1377, April 2011.
69. C.-Y. Sue and N.-C. Tsai. Human powered MEMS-based energy harvest devices. *Applied Energy* **93**:390–403, 2012.
70. C. Xu, C. Pan, Y. Liu, and Z. L. Wang. Hybrid cells for simultaneously harvesting multi-type energies for self-powered micro/nanosystems. *Nano Energy* **1**(2):259–272, 2012.
71. F. Davis and S. P. J. Higson. Biofuel cells-recent advances and applications. *Biosensors and Bioelectronics* **22**(7):1224–1235, 2007.
72. C. B. Williams, C. Shearwood, M. A. Harradine, P. H. Mellor, T. S. Birch, and R. B. Yates. Development of an electromagnetic micro-generator. *Proceedings of the IEEE Circuits, Devices and Systems* **148**(6):337–342, 2001.

73. B. J. Hansen, Y. Liu, R. Yang, and Z. L. Wang. Hybrid nanogenerator for concurrently harvesting biomechanical and biochemical energy. *ACS Nano* **4**(7):3647–3652, 2010.
74. S. Sherrit. The physical acoustics of energy harvesting. In *Proceedings of IEEE IUS 2008*, November 2008, pp. 1046–1055.
75. F. Liu, A. Phipps, S. Horowitz, K. Ngo, L. Cattafesta, T. Nishida, and M. Sheplak. Acoustic energy harvesting using an electromechanical Helmholtz resonator. *Journal of the Acoustical Society of America* **123**(4):1983–1990, 2008.
76. T. T. Le. *Efficient power conversion interface circuits for energy harvesting applications*. PhD thesis, Oregon State University, April 2008.
77. A. Denisov and E. Yeatman. Stepwise microactuators powered by ultrasonic transfer. In *Proceedings of the Eurosensors XXV*, Athens, Greece, September 2011.
78. Y. Zhu, S. O. R. Moheimani, and M. R. Yuce. A 2-DOF MEMS ultrasonic energy harvester. *IEEE Sensors Journal* **11**(1):155–161, 2011.
79. M. Belleville, H. Fanet, P. Fiorini, P. Nicole, M. J. M. Pelgrom, C. Piguet, R. Hahn, C. Van Hoof, R. Vullers, M. Tartagni, and E. Cantatore. Energy autonomous sensor systems: Towards a ubiquitous sensor technology. *Microelectronics Journal* **41**(11): 740–745, 2010.
80. R. J. M. Vullers, R. van Schaijk, I. Doms, C. Van Hoof, and R. Mertens. Micropower energy harvesting. *Solid-State Electronics* **53**(7):684–693, 2009.
81. L. Huang, V. Pop, R. de Francisco, R. Vullers, G. Dolmans, H. de Groot, and K. Imamura. Ultra low power wireless and energy harvesting technologies - an ideal combination. In *Proceedings of IEEE ICCS 2010*, November 17–19, 2010, pp. 295–300.
82. P. Mane, J. Xie, K. K. Leang, and K. Mossi. Cyclic energy harvesting from pyroelectric materials. *IEEE Transactions on Ultrasonics, Ferroelectrics and Frequency Control* **58**(1):10–17, 2011.
83. J. A. Paradiso and T. Starner. Energy scavenging for mobile and wireless electronics. *IEEE Pervasive Computing* **4**(1):18–27, 2005.
84. S. P. Beeby, R. N. Torah, M. J. Tudor, P. Glynne-Jones, T. O'Donnell, C. R. Saha, and S. Roy. A micro electromagnetic generator for vibration energy harvesting. *Journal of Micromechanics and Microengineering* **17**(7):1257–1265, 2007.
85. S. Roundy, E. S. Leland, J. Baker, E. Carleton, E. Reilly, E. Lai, B. Otis, J. M. Rabaey, P. K. Wright, and V. Sundararajan. Improving power output for vibration-based energy scavengers. *IEEE Pervasive Computing* **4**(1):28–36, January–March 2005.
86. M. Bolić, D. Simplot-Ryl, and I. Stojmenović. *Rfid Systems: Research Trends and Challenges*. John Wiley & Sons, Hoboken, NJ, 2010.
87. M. A. Green, K. Emery, Y. Hishikawa, and W. Warta. Solar cell efficiency tables (version 37). *Progress in Photovoltaics: Research and Applications* **19**(1):84–92, 2011.
88. D. Vanderpool, J. H. Yoon, and L. Pilon. Simulations of a prototypical device using pyroelectric materials for harvesting waste heat. *International Journal of Heat and Mass Transfer* **51**(21):5052–5062, 2008.
89. Powercast. http://www.powercast.com., 2011.
90. D. R. Cox. Prediction by exponentially weighted moving averages and related methods. *Journal of the Royal Statistical Society. Series B (Methodological)* **23**(2):414–422, 1961.
91. J. R. Piorno, C. Bergonzini, D. Atienza, and T. S. Rosing. Prediction and management in energy harvested wireless sensor nodes. In *Proceedings of Wireless VITAE 2009*, May 17–20, 2009, pp. 6–10.

92. C. Bergonzini, D. Brunelli, and L. Benini. Comparison of energy intake prediction algorithms for systems powered by photovoltaic harvesters. *Microelectronics Journal* **41**(11):766–777, 2010.

93. C. Moser, L. Thiele, D. Brunelli, and L. Benini. Adaptive power management in energy harvesting systems. In *Proceedings of DATE 2007*, April 2007, pp. 1–6.

94. D. K. Noh and K. Kang. Balanced energy allocation scheme for a solar-powered sensor system and its effects on network-wide performance. *Journal of Computer and System Sciences* **77**(5):917–932, 2011.

95. D. Spenza and C. Petrioli. Pro-energy, a novel energy prediction model for solar and wind energy harvesting WSNs. Poster at the N2Women Workshop, co-located with IEEE Infocom 2012, Orlando, FL, March 26, 2012.

96. N. Sharma, J. Gummeson, D. Irwin, and P. Shenoy. Cloudy computing: Leveraging weather forecasts in energy harvesting sensor systems. In *Proceedings of SECON 2010*, Boston, MA, June 21–25, 2010, pp. 1–9.

Q1 97. S. Liu, J. Lu, Q. Wu, and Q. Qiu. Harvesting-aware power management for real-time systems with renewable energy. *IEEE Transactions on Very Large Scale Integration (VLSI) Systems*, 2012.

98. S. Liu, Q. Wu, and Q. Qiu. An adaptive scheduling and voltage/frequency selection algorithm for real-time energy harvesting systems. In *Proceedings of ACM/IEEE DAC 2009*, July 2009, pp. 782–787.

99. A. Ravinagarajan, D. Dondi, and T. S. Rosing. DVFS based task scheduling in a harvesting WSN for structural health monitoring. In *Proceedings of DATE 2010*, Leuven, Belgium, March 8–12, 2010, pp. 1518–1523.

100. J. Recas Piorno, C. Bergonzini, D. Atienza Alonso, and T. S. Rosing. HOLLOWS: A power-aware task scheduler for energy harvesting sensor nodes. *Journal of Intelligent Material Systems and Structures* **21**(12):1317–1335, 2010.

101. C. Rusu, R. Melhem, and D. Mossé. Multi-version scheduling in rechargeable energy-aware real-time systems. *Journal of Embedded Computing* **1**(2):271–283, 2005.

102. J. B. Steck and T. S. Rosing. Adapting task utility in externally triggered energy harvesting wireless sensing systems. In *Proceedings of INSS 2009*, June 2009, pp. 1–8.

103. C. Moser, D. Brunelli, L. Thiele, and L. Benini. *Lazy Scheduling for Energy Harvesting Sensor Nodes*, Vol. 225 of *IFIP International Federation for Information Processing*, Springer, October 2006, pp. 125–134.

104. C. Moser, D. Brunelli, L. Thiele, and L. Benini. Real-time scheduling with regenerative energy. In *Proceedings of ECRTS 2006*, July 2006, pp. 261–270.

105. D. Audet, L. C. de Oliveira, N. MacMillan, D. Marinakis, and K. Wu. Scheduling recurring tasks in energy harvesting sensors. In *Proceedings of IEEE INFOCOM 2011 Workshop on Green Communication and Networking*, April 2011, pp. 277–282.

106. H. EL Ghor, M. Chetto, and R. H. Chehade. A real-time scheduling framework for embedded systems with environmental energy harvesting. *Computers and Electrical Engineering Journal* **37**(4):498–510, 2011.

107. S. Liu, Q. Qiu, and Q. Wu. Energy aware dynamic voltage and frequency selection for real-time systems with energy harvesting. In *Proceedings of DATE 2008*, March 2008, pp. 236–241.

108. A. Bar-Noy, T. Brown, M. P. Johnson, T. F. La Porta, O. Liu, and H. Rowaihy. Assigning sensors to missions with demands. In *Algorithmic Aspects of Wireless Sensor Networks*,

Vol. 4837 of *Lecture Notes in Computer Science*, M. Kutylowski, J. Cichon, and P. Kubiak, Eds. Springer, New York, 2008, pp. 114–125.

109. M. P. Johnson, H. Rowaihy, D. Pizzocaro, A. Bar-Noy, S. Chalmers, T. La Porta, and A. Preece. Sensor-mission assignment in constrained environments. *IEEE Transactions on Parallel and Distributed Systems* **21**(11):1692–1705, 2010.
110. H. Rowaihy, M. P. Johnson, A. Bar-Noy, T. Brown, and T. F. La Porta. Assigning sensors to competing missions. In *Proceedings of IEEE GLOBECOM 2008*, November 30–December 4, 2008, pp. 1–6.
111. H. Rowaihy, M. P. Johnson, D. Pizzocaro, A. Bar-Noy, L. M. Kaplan, T. F. La Porta, and A. D. Preece. Detection and localization sensor assignment with exact and fuzzy locations. In *Proceedings of DCOSS 2009*, Marina del Rey, CA, 2009, pp. 28–43.
112. T. La Porta, C. Petrioli, and D. Spenza. Sensor-mission assignment in wireless sensor networks with energy harvesting. In *Proceedings of IEEE SECON 2011*, Seoul, Korea, June 18–21, 2011, pp. 413–421.
113. X. Fafoutis and N. Dragoni. ODMAC: An on-demand MAC protocol for energy harvesting wireless sensor networks. In *Proceedings of ACM PE-WASUN 2011*, November 3–4, 2011, pp. 49–56.
114. J. Kim and J.-W. Lee. Energy adaptive MAC protocol for wireless sensor networks with RF energy transfer. In *Proceedings of IEEE ICUFN 2011*, June 2011, pp. 89–94.
115. J. Kim and J.-W. Lee. Performance analysis of the energy adaptive MAC protocol for wireless sensor networks with RF energy transfer. In *Proceedings of IEEE ICTC 2011*, September 2011, pp. 14–19.
116. C. Fujii and W. K. G. Seah. Multi-tier probabilistic polling for wireless sensor networks powered by energy harvesting. In *Proceedings of IEEE ISSNIP 2011*, December 2011.
117. Z. A. Eu, H.-P. Tan, and W. K. G. Seah. Design and performance analysis of MAC schemes for wireless sensor networks powered by ambient energy harvesting. *Ad Hoc Network* **9**(3):300–323, 2011.
118. IEEE 802.15.4-2006 Standard. Wireless medium access control (MAC) and physical layer (PHY) specifications for low-rate wireless personal area networks (WPANs), 2006.
119. Z. A. Eu, W. K. G. Seah, and H.-P. Tan. A study of MAC schemes for wireless sensor networks powered by ambient energy harvesting. In *Proceedings of WICON 2008*, Maui, Hawaii, 2008, pp. 78:1–78:9.
120. F. Iannello, O. Simeone, and U. Spagnolini. Medium access control protocols for wireless sensor networks with energy harvesting. *IEEE Transactions on Communications*, 2012. **Q1**
121. S. Basagni, M. Nati, C. Petrioli, and R. Petroccia. ROME: Routing over mobile elements in WSNs. In *Proceedings of IEEE GLOBECOM 2009*, Honolulu, Hawaii, November 30–December 4 2009, pp. 1–7.
122. A. Camilló, M. Nati, C. Petrioli, M. Rossi, and M. Zorzi. IRIS: Integrated data gathering and interest dissemination system for wireless sensor networks. *Ad Hoc Networks*, 2012. Special issue on cross layer design. To appear. **Q1**
123. P. Casari, M. Nati, C. Petrioli, and M. Zorzi. ALBA: An adaptive load-balanced algorithm for geographic forwarding in wireless sensor networks. In *Proceedings of IEEE MILCOM 2006*, Washington, DC, October 23–25, 2006, pp. 1–9.
124. D. Ferrara, L. Galluccio, A. Leonardi, G. Morabito, and S. Palazzo. MACRO: An integrated MAC/routing protocol for geographic forwarding in wireless sensor networks.

In *Proceedings of IEEE INFOCOM 2005*, Vol. 3, Miami, FL, March 13–17, 2005, pp. 1770–1781.

125. M. C. Vuran and I. F. Akyildiz. XLP: A cross-layer protocol for efficient communication in wireless sensor networks. *IEEE Transactions on Mobile Computing* **9**(11):1578–1591, 2010.
126. M. Zorzi and R. R. Rao. Geographic random forwarding (GeRaF) for ad hoc and sensor networks: Energy and latency performance. *IEEE Transactions on Mobile Computing* **2**(4):349–365, 2003.
127. E. Lattanzi, E. Regini, A. Acquaviva, and A. Bogliolo. Energetic sustainability of routing algorithms for energy-harvesting wireless sensor networks. *Computer Communications* **30**(14–15):2976–2986, 2007.
128. N. Pais, B. K. Cetin, N. Pratas, F. J. Velez, N. R. Prasad, and R. Prasad. Cost-benefit aware routing protocol for wireless sensor networks with hybrid energy storage system. *Journal of Green Engineering* **1**(2):189–208, 2011.
129. P. K. K. Loh, S. H. Long, and Y. Pan. An efficient and reliable routing protocol for wireless sensor networks. In *Proceedings of WoWMoM 2005*, June 2005, pp. 512–516.
130. M. K. Jakobsen, J. Madsen, and M. R. Hansen. DEHAR: A distributed energy harvesting aware routing algorithm for ad-hoc multihop wireless sensor networks. In *Proceedings of WoWMoM 2010*, June 2010, pp. 1–9.
131. Z. A. Eu, H.-P. Tan, and W. K. G. Seah. Opportunistic routing in wireless sensor networks powered by ambient energy harvesting. *Computer Networks* **54**(17):2943–2966, December 2010.
132. D. Noh and I. Yoon. Low-latency geographic routing for asynchronous energy-harvesting WSNs. *Journal of Networks* **3**(1):78–85, 2008.
133. L. Lin, N. B. Shroff, and R. Srikant. Asymptotically optimal energy-aware routing for multihop wireless networks with renewable energy sources. *IEEE/ACM Transactions on Networking* **15**(5):1021–1034, October 2007.
134. A. Bogliolo and E. Lattanzi. Energetic sustainability of environmentally powered wireless sensor networks. In *Proceedings of ACM PE-WASUN 2006*, Torremolinos, Spain, October 2–6, 2006, pp. 149–152.
135. D. Hasenfratz, A. Meier, C. Moser, J.-J. Chen, and L. Thiele. Analysis, comparison, and optimization of routing protocols for energy harvesting wireless sensor networks. In *Proceedings of SUTC 2010*, June 2010, pp. 19–26.
136. K. Zeng, K. Ren, W. Lou, and P. J. Moran. Energy-aware geographic routing in lossy wireless sensor networks with environmental energy supply. *ACM Wireless Networks (WINET)* **15**(1):39–51, 2009.
137. R. Doost, K. R. Chowdhury, and M. Di Felice. Routing and link layer protocol design for sensor networks with wireless energy transfer. In *Proceedings of IEEE GLOBECOM 2010*, December 2010, pp. 1–5.
138. I. D. Chakeres and E. M. Belding-Royer. AODV routing protocol implementation design. In *Proceedings of WWAN 2004*, Tokyo, Japan, March 23–24, 2004, pp. 698–703.

Author Query

Q1 Update.